A gPC-based approach to uncertain interaction of oblique shocks and supersonic mixing layers

Sarah Baaziz *
University of Lille, Lille Fluid Mechanics Laboratory, France

Nabil El Moçayd †
Mohammed VI Polytechnic University (UM6P), IWRI Group, Benguerir, Morocco

Radouan Boukharfane ‡
Mohammed VI Polytechnic University (UM6P), MSDA Group, Benguerir, Morocco

The present paper focus on the stochastic response of a two-dimensional shock wave impingement on a spatially evolving mixing layer to parametric uncertainties. Both the oblique shock angle and the convective Mach number are considered as random parameters and the generalized Polynomial Chaos (gPC) theory is coupled with standard deterministic numerical simulations through a spectral collocation projection methodology. In this framework, the two input parameters investigated are considered as random variables with a given probability distribution over the range of investigation prescribed. The uncertainty is then propagated through the computational model to statistically quantify their effect on the results. This study allows for a better understanding of the flow sensitivity to such uncertainties and underline the coupling process between the stochastic parameters. Some results of direct numerical simulations of the multicomponent, compressible, reactive Navier-Stokes equations are reported here for the particular case of a two-dimensional mixing layer. Special emphasis is placed on the effects associated with heat release.

I. Introduction

The validation and verification of computational fluid dynamics (CFD) tools using wind tunnel experimental results poses many questions on the way to setup the test case and on the necessary test data to use in the numerical configuration to make the numerical simulation most compatible to the real flow [1]. In this process the account of real information on the flow generated by the wind tunnel appears as an important matter often neglected in the simulation work. In fact a wind tunnel represents a complex system that generates testing conditions not necessarily well-known [2]. This leads to an intrinsic uncertainty in the proper setting and initialisation of the numerical model to target experimental reproduction that, on general grounds, includes geometrical and flow parameters alike. In this work, the system of interest is the interactions of shocks with shear flows which occur in many high-speed flow situations such as external aerodynamics of transonic, supersonic and hypersonic flow, internal flows in scramjets [3, 4]. Shock interactions with free shear and wall-bounded flows have been shown to impact mixing, increase losses and affect surface drag and/or heat transfer depending upon the strength of the shock. Uncertainty quantification of the influence of uncertain

---

*Graduate Student, sarah.baaziz@um6p.ma
†Assistant professor, nabil.elmocayd@um6p.ma
‡Research & Education fellow, radouan.boukharfane@um6p.ma, AIAA Member

parameters onto mixing efficiency obtained from shock/shear interactions is a major issue in order to properly predict the system response to random inputs. Several benefits can be gained from such studies. For example, it permits to i) take into consideration realistic safety margins depending on the solution sensitivity to the random inputs, and ii) to study the coupling process between several uncertain parameters, which can not be investigated through linearized approaches like Adjoint-state-based methods [5]. Moreover, uncertainty quantification leads to a classification of the most influential parameters on the system response and allows for the identification of extreme behaviors under specific coupling. Moreover, uncertainty quantification leads to a classification of the most influential parameters on the system response. A better understanding of the related phenomena is thus required for applications such as scramjet engines, the efficiency of which depends crucially on a proper mixing of oxidizer and fuel. In the present study, the effects of a randon oblique shock angle and convective Mach number on the mean flow are examined. The influence of the turbulent structures on the global interaction is then identified, and the mixing enhancement is assessed. The analysis is conducted in the light of DNS results.

II. Description of the numerical solver

The unsteady, compressible Navier-Stokes equations are considered for a multi-species reactive gas mixture:

$$\frac{\partial \rho}{\partial t} + \frac{\partial \rho u_j}{\partial x_j} = 0, \tag{1}$$

$$\frac{\partial \rho u_i}{\partial t} + \frac{\partial \rho u_i u_j}{\partial x_j} + \frac{\partial p}{\partial x_i} = \frac{\partial \tau_{ij}}{\partial x_j}, \quad i \in [1, 3], \tag{2}$$

$$\frac{\partial \rho e_t}{\partial t} + \frac{\partial (\rho e_t + p) u_j}{\partial x_j} = \frac{\partial u_j \tau_{ij}}{\partial x_j} - \frac{\partial q_j}{\partial x_j}, \tag{3}$$

$$\frac{\partial \rho Y_\alpha}{\partial t} + \frac{\partial \rho Y_\alpha u_j}{\partial x_j} = -\frac{\partial \rho Y_\alpha V_{\alpha j}}{\partial x_j} + \rho \dot{\omega}_\alpha, \quad \alpha \in [1, \mathcal{N}_{sp}], \tag{4}$$

where $\tau_{ij} = 2\mu \left(S_{ij} - \delta_{ij} S_{kk}/3 \right)$ and $S_{ij} = \left(\partial u_i/\partial x_j + \partial u_j/\partial x_i \right)/2$. $\rho e_t = \rho u_i u_i/2 + \rho \sum_{\alpha=1}^{\mathcal{N}_{sp}} h_\alpha Y_\alpha - p$ and $h_\alpha (T_1) = \Delta h_{f\,\alpha}^0 + \int_{T_0}^{T_1} c_{p\alpha} (T) \, dT$. The pressure of the mixture is given by $p = \rho \mathcal{R} T / \mathcal{W}$, with $\mathcal{W}^{-1} = \sum_{\alpha=1}^{\mathcal{N}_{sp}} Y_\alpha / \mathcal{W}_\alpha$. $q_j = -\lambda \partial T/\partial x_j + \rho \sum_{\alpha=1}^{\mathcal{N}_{sp}} h_\alpha Y_\alpha V_{\alpha j}$ and $Y_\alpha V_{\alpha j} = Y_\alpha \sum_{\beta=1}^{\mathcal{N}_{sp}} D_\beta (\mathcal{W}_\beta/\mathcal{W}) \partial X_\beta/\partial x_j - D_\alpha (\mathcal{W}_\alpha/\mathcal{W}) \partial X_\alpha/\partial x_j$. This system of conservative equations is based on the following set of independent variables: the density ρ, the momentum ρu_i, the mass fraction of the $\mathcal{N}_{sp}$ species ρY_α and the total energy ρe_t. Each species behaves as a thermally perfect gas with its thermodynamic properties determined from the JANAF databases [6]. The viscosity μ and thermal conductivity λ depend on the temperature of the mixture as well as its composition. The mixture diffusion coefficients D_α depend on the temperature and pressure of the mixture but the Dufour and Soret effects are not taken into account. The mass production terms $\dot{\omega}_\alpha$ are derived from a set of chemical reaction equations which are expressed in terms of an Arrhenius temperature dependence form, making possible the use of detailed chemical kinetic mechanisms.

The treatment of the advective terms in the transport equations relies on a solution-adaptive finite-difference method whereby different numerical schemes are applied for shocks and broadband turbulence. Narrow regions around shock waves are treated with a nonlinear upwinding seventh-order accurate weighted essentially non-oscillatory (WENO-Z) scheme of Don and Borges [7] with Roe flux splitting, whereas the underlying seventh-order upwind discretization is

used elsewhere by disabling the nonlinear weights. At each time step, shocks are detected based on Ducros [8] shock sensor which is activated if

$$\partial_i u_i > 0.7 \sqrt{(\partial_i u_i)^2 + \Omega^2}, \tag{5}$$

where Ω^2 is a low-pass-filtered vorticity magnitude. The viscous and molecular diffusion fluxes are discretized using eighth-order centered finite difference formulas. Time integration is carried out by means of a third-order total variation diminishing (TVD) Runge–Kutta algorithm [9]. The time step is set such that the acoustic Courant-Friedrichs-Lewy (CFL) number does not exceed 0.5. The enthalpies and the specific heat capacities of each species are expressed as polynomial functions of temperature using the JANAF tables [6]. The above mentioned transport coefficients, *i.e.*, κ, μ, $\widetilde{\mathcal{D}}_{\alpha,\beta}$ and $\tilde{\chi}_\beta$, which are functions of the temperature and the mixture, are evaluated using the general purpose FORTRAN library EGLIB [10]. The supersonic streams of hydrogen/air consists of nine species (H_2, O_2, H, O, OH, HO_2, H_2O_2, H_2O, N_2). To speed up the simulations of the inert cases, the intermediate species are neglected and the mass fraction of N_2 is slightly modified to guarantee mass conservation. A detailed verification of the solver may be found in [11].

III. Generalized polynomial chaos

The main features of the generalized polynomial chaos approach are briefly recalled here; for more details we refer to Ghanem and Spanos [12] and Le Maître and Knio [13]. In the last years, this stochastic approach has been applied to turbulent flow analysis with satisfying results [14]. Define a *probability space* $(\Omega, \mathcal{A}, \mathcal{P})$ where Ω is the event space, $\mathcal{A} \subset 2^\Omega$ its σ-algebra and $\mathcal{P}$ its probability measure. Being ω an element of the event space, we define a random field $X(\omega)$ such that it maps the probability space into a function space V, $X : \Omega \to V$. In the following we will consider second-order random fields, *i.e.*, those satisfying the relation $\mathbf{E}(X, X) < +\infty$, where $\mathbf{E}$ denotes the expectation of a random variable. In this context, gPC is a tool allowing second-order random fields to be represented through a set of random variables $\xi(\omega)$. An approximation of the random field $X(\omega)$ is then recovered through its Galerkin projection onto a polynomial orthogonal basis taking the following form:

$$X(\omega) = a_0 B_0 + \sum_{i_1=1}^{\infty} a_{i_1} B_1(\xi_{i_1}) + \sum_{i_1=1}^{\infty} \sum_{i_2=1}^{i_1} a_{i_1 i_2} B_2(\xi_{i_1}, \xi_{i_2}) + ..., \tag{6}$$

where $\xi = (\xi_1, ..., \xi_N)^T$ is a N-dimensional random vector and B_i is a polynomial of order i depending on the σ algebra of ξ. This expression can be easily reformulated using a term-based indexing instead of a order-based indexing. Let $\Phi_k(\xi(\omega))$ be a single polynomial, the pseudospectral approximation (6) can be written as follows:

$$X(\omega) = \sum_{k=0}^{\infty} a_k \Phi_k(\xi(\omega)), \tag{7}$$

in which there is a one-to-one correspondence between $a_{i_1 i_2 \cdots I_n}$ and a_k and between $B_n(\xi_{i_1}, \xi_{i_2}, \cdots, \xi_{i_n})$ and $\Phi_k(\xi)$ The polynomial expansion is truncated to a finite limit and the orthogonality of the polynomials is set through the relation $\langle \Phi_i \Phi_j \rangle = \langle \Phi_i^2 \rangle \delta_{ij}$, where $\langle \cdot, \cdot \rangle$ denotes an ensemble average. This inner product is defined over the measure

$W(\xi)$ of the random variables as follows:

$$\langle f(\xi)g(\xi)\rangle = \int_{\omega \in \Omega} f(\xi)g(\xi)dP(\omega) = \int f(\xi)g(\xi)W(\xi)d\xi. \tag{8}$$

Thanks to the orthogonality of the polynomial basis, each coefficient of the Galerkin projection (7) can be recovered through the following definition:

$$a_k = \frac{\langle X, \Phi_k \rangle}{\langle \Phi_k^2 \rangle} = \frac{1}{\langle \Phi_k^2 \rangle} \int_{\omega \in \Omega} X \Phi_k \rho(\xi)d(\xi), \tag{9}$$

where each inner product involves a multidimensional integral over the support range of the weighting function. The integrals can be computed through different mathematical methods: considering the number of random variables investigated, the coefficients a_k have been computed through Gaussian quadrature in the present work.

The polynomial family to be used must be a priori specified. The choice of the polynomials affects the speed of the convergence of the series: a unsuitable polynomial family may lead to the need of a large number of degrees of freedom to obtain a given level of accuracy (*i.e.* a higher order of the polynomials), while a suitable polynomials family is able to interpolate both the input and the random variables by means of a few degrees of freedom. In the case of the input, when dealing with Gaussian quadrature, an optimal family has a weight coefficient similar to the function W. The probability density function PDF of the random variables has been considered as *uniform* leading to the choice of the Legendre polynomial family: this is a well suited choice since the inner product weighting function is directly proportional with a factor 0.5 to the set probability density function. The polynomial expansion has been limited to the third order since the contribution of fourth and higher order polynomials is negligible. This leads to the use of a 20 polynomial basis to generate the error cost function over the uncertainty space. The gPC application is herein used in its non-intrusive approach, *i.e.*, the variables, and more precisely the error cost functions are directly projected over the orthogonal basis spanning the random space, without any modification of the deterministic solver. The number of points to discretize each random variable space is chosen in order to recover converged integrals when computing the polynomial coefficients. **The polynomial expansion being truncated to the third order, 5 points for each random variable are sufficient to compute the coefficients a_k.**

IV. Problem statement and computational setup

The upper stream corresponds to the fuel inlet, *i.e.*, a mixture containing hydrogen, and the bottom inlet stream to vitiated air. A typical sketch of the corresponding computational geometry is provided in Fig. 1 and the main parameters relevant to the present numerical simulation are given in Tab. 1. Assuming equal free-stream specific heat capacity ratios, the convective Mach number may be evaluated from $M_c = (U_1 - U_2)/(a_1 + a_2)$, where a_1 and a_2 denotes the sonic speeds of streams 1 (oxidizer inlet stream) and 2 (fuel inlet stream) respectively. The values of the velocity at the inlets are $U_1 = 1634$ m/s at bottom (oxidizer stream) and U_2 (fuel stream) is determined once the value of M_c is imposed. The mixing layer flow is impinged by an oblique shock wave that is issued from the oxidizer inlet stream at the bottom boundary. The geometrical parameters relevant to the present set of numerical simulations are $L_{x_1} = 280$ and $L_{x_2} = 130$, which denote the computational domain lengths in each direction normalized by the initial vorticity thickness $\delta_{\omega,0} = 1.44 \times 10^{-4}$ m, and $N_{x_1} = 1640$ and $N_{x_2} = 750$, which are the corresponding numbers of grid points. The flow is
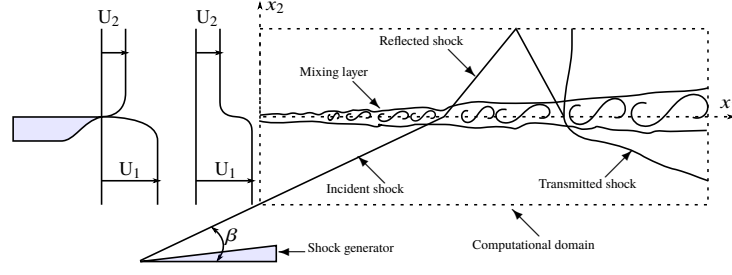
Fig. 1   Sketch of the two-dimensional shock–mixing layer interaction geometry.

Simulation no.	β (°)	Mach convective M_c (-)	Fuel U_2 (m/s)	Oxidizer U_1 (m/s)	Re_{δ_ω} (-)
1	30.47	0.32	1194.44	1634	425.79
2	30.47	0.39	1093.02	1634	524.03
3	30.47	0.50	944.52	1634	667.88
4	30.47	0.61	796.01	1634	811.73
5	30.47	0.68	694.59	1634	909.98
6	32.31	0.32	1194.44	1634	425.79
7	32.31	0.39	1093.02	1634	524.03
8	32.31	0.50	944.52	1634	667.88
9	32.31	0.61	796.01	1634	811.73
10	32.31	0.68	694.59	1634	909.98
11	35.00	0.32	1194.44	1634	425.79
12	35.00	0.39	1093.02	1634	524.03
13	35.00	0.50	944.52	1634	667.88
14	35.00	0.61	796.01	1634	811.73
15	35.00	0.68	694.59	1634	909.98
16	37.69	0.32	1194.44	1634	425.79
17	37.69	0.39	1093.02	1634	524.03
18	37.69	0.50	944.52	1634	667.88
19	37.69	0.61	796.01	1634	811.73
20	37.69	0.68	694.59	1634	909.98
21	39.53	0.32	1194.44	1634	425.79
22	39.53	0.39	1093.02	1634	524.03
23	39.53	0.50	944.52	1634	667.88
24	39.53	0.61	796.01	1634	811.73
25	39.53	0.68	694.59	1634	909.98

Tab. 1   Database of DNS simulations used in the present analysis. Results from simulations 1-25 are used to reconstruct the response surfaces of the stochastic quantities analysed, by the use of a non-intrusive gPC approach.

initialized with a hyperbolic tangent profile for the streamwise velocity component, while the other velocity components are set at zero. Species mass fractions and density are also set according to the following general expression:

$$\varphi(x_1, x_2, x_3) = \frac{\varphi_1 + \varphi_2}{2} + \frac{\varphi_1 - \varphi_2}{2} \tanh\left(\frac{2x_2}{\delta_{\omega,0}}\right), \tag{10}$$

where φ denotes any of the flow variables mentioned above (i.e., species mass fraction or streamwise velocity component). The value of the Reynolds number Re_{δ_ω} is based on the initial vorticity thickness and inlet velocity difference $\Delta U = U_1 - U_2$. One of the fundamental statistical quantities that characterizes the mixing layer development is its normalized growth rate [15]. Although the definition of this growth rate is not unique, one standard expression

relies on the vorticity thickness definition [16]:

$$\delta_\omega(x_1) = \frac{U_1 - U_2}{\partial \widetilde{u}_1 / \partial x_2 |_{\max}} \tag{11}$$

Dirichlet boundary conditions are applied at the two supersonic inlets, perfectly non-reflecting boundary conditions are set at the outflow. A slip boundary condition is imposed at the top, while the bottom boundary condition is set by using Rankine-Hugoniot relations, generalized for a multicomponent mixture [17]. In order to trigger flow transition, a slight white noise fluctuation is superimposed to the transverse velocity component along the line $(x_1, x_2) = (4\delta_{\omega,0}, 0)$. The value of the CFL number is set to 0.75. Reactive flow simulations are conducted with the detailed mechanism of O'Conaire et al. [18]. It consists of nine chemical species (H_2, O_2, H_2O, H, O, OH, HO_2, H_2O_2, and N_2) and 21 elementary reaction steps. The concentrations of these species at the inlet have been determined from equilibrium conditions so as to reach favorable self-ignition conditions within the extension of the computational domain.

Throughout this manuscript, the Reynolds and Favre averages of any quantity φ are denoted by $\overline{\varphi}$ and $\widetilde{\varphi}$, while the corresponding statistical fluctuations are denoted by single and double primes, i.e., φ' and φ'', respectively. Averaging is performed over the direction of statistical homogeneity and time t.

References

[1] Szoke, M., Vishwanathan, V., Loeschen, T., Gargiulo, A., Fritsch, D. J., Duetsch-Patel, J. E., Borgoltz, A., Roy, C. J., Lowe, K. T., and Devenport, W. J., "Developing a numerical model of the Virginia Tech stability wind tunnel for uncertainty quantification based on real-world geometry," *AIAA Scitech 2020 Forum*, 2020, p. 0343.

[2] Cattafesta, L., Bahr, C., and Mathew, J., "Fundamentals of wind-tunnel design," *Encyclopedia of Aerospace Engineering*, 2010, pp. 1–10.

[3] Chakravarthy, R. V. K., Nair, V., Muruganandam, T. M., and Ghosh, S., "Analytical and numerical study of normal shock response in a uniform duct," *Physics of Fluids*, Vol. 30, No. 8, 2018, p. 086101.

[4] Karthick, S. K., "Shock and shear layer interactions in a confined supersonic cavity flow," *Physics of Fluids*, Vol. 33, No. 6, 2021, p. 066102.

[5] Mittal, A., Chen, X., Tong, C. H., and Iaccarino, G., "A flexible uncertainty propagation framework for general multiphysics systems," *SIAM/ASA Journal on Uncertainty Quantification*, Vol. 4, No. 1, 2016, pp. 218–243.

[6] Prophet, H., Stull, D. R., United States, and National Bureau of Standards, *JANAF thermochemical tables*, U.S. Dept. of Commerce, National Bureau of Standards, 1971.

[7] Don, W.-S., and Borges, R., "Accuracy of the weighted essentially non–oscillatory conservative finite difference schemes," *Journal of Computational Physics*, Vol. 250, 2013, pp. 347–372.

[8] Ducros, F., Ferrand, V., Nicoud, F., Weber, C., Darracq, D., Gacherieu, C., and Poinsot, T., "Large-eddy simulation of the shock/turbulence interaction," *Journal of Computational Physics*, Vol. 152, No. 2, 1999, pp. 517–549.

[9] Gottlieb, S., and Shu, C.-W., "Total variation diminishing Runge–Kutta schemes," *Mathematics of Computation*, Vol. 67, No. 221, 1998, pp. 73–85.

[10] Ern, A., and Giovangigli, V., "EGLIB: A general-purpose fortran library for multicomponent transport property evaluation," Technical report, CERMICS, 2004.

[11] Boukharfane, R., "Contribution à la simulation numérique d'écoulements turbulents compressibles canoniques," Ph.D. thesis, École Nationale Supérieure de Mécanique et d'Aérotechnique, 2018.

[12] Ghanem, R. G., and Spanos, P. D., *Stochastic finite elements: a spectral approach*, Courier Corporation, 2003.

[13] Le Maître, O., and Knio, O. M., *Spectral methods for uncertainty quantification: with applications to computational fluid dynamics*, Springer Science & Business Media, 2010.

[14] Lucor, D., Meyers, J., and Sagaut, P., "Sensitivity analysis of large-eddy simulations to subgrid-scale-model parametric uncertainty using polynomial chaos," *Journal of Fluid Mechanics*, Vol. 585, 2007, pp. 255–279.

[15] Ramshaw, J. D., "Simple model for mixing at accelerated fluid interfaces with shear and compression," *Physical Review E*, Vol. 61, No. 5, 2000, p. 5339.

[16] Pantano, C., Sarkar, S., and Williams, F. A., "Mixing of a conserved scalar in a turbulent reacting shear layer," *Journal of Fluid Mechanics*, Vol. 481, 2003, pp. 291–328.

[17] Mitchell, R. E., and Kee, R. J., "A general-purpose computer code for predicting chemical-kinetic behavior behind incident and reflected shocks," *NASA STI/Recon Technical Report N*, Vol. 83, 1982, p. 27169.

[18] Ó Conaire, M., Curran, H. J., Simmie, J. M., Pitz, W. J., and Westbrook, C. K., "A comprehensive modeling study of hydrogen oxidation," *International Journal of Chemical Kinetics*, Vol. 36, No. 11, 2004, pp. 603–622.